Environ. Sci. Technol. **2002**, *36,* 5041−5050

Ultrafine PM Emissions from Natural Gas, Oxidation-Catalyst Diesel, and Particle-Trap Diesel Heavy-Duty Transit Buses

BRITT A. HOLMÉN*,† AND ALBERTO AYALA‡

Civil and Environmental Engineering, University of Connecticut, Storrs, Connecticut 06269-2037, and California Environmental Protection Agency, Air Resources Board, Sacramento, California 95812

This paper addresses how current technologies effective for reducing PM emissions of heavy-duty engines may affect the physical characteristics of the particles emitted. Three in-use transit bus configurations were compared in terms of submicron particle size distributions using simultaneous SMPS measurements under two dilution conditions, a minidiluter and the legislated constant volume sampler (CVS). The compressed natural gas (CNG) -fueled and diesel particulate filter (DPF) -equipped diesel configurations are two "green" alternatives to conventional diesel engines. The CNG bus in this study did not have an oxidation catalyst, whereas the diesel configurations (with and without particulate filter) employed catalysts. The DPF was a continuously regenerating trap (CRT). Particle size distributions were collected between 6 and 237 nm using 2-minute SMPS scans during idle and 55 mph steady-state cruise operation. Average particle size distributions collected during idle operation of the diesel baseline bus operating on ultralow sulfur fuel showed evidence for nanoparticle growth under CVS dilution conditions relative to the minidiluter. The CRT effectively reduced both accumulation and nuclei mode concentrations by factors of 10−100 except under CVS dilution conditions where nuclei mode concentrations were measured during 55 mph steady-state cruise that exceeded baseline diesel concentrations. The CVS data suggest some variability in trap performance. The CNG bus had accumulation mode concentrations 10−100× lower than the diesel baseline but often displayed large nuclei modes, especially under CVS dilution conditions. Partly this may be explained by the lack of an oxidation catalyst on the CNG, but differences between the minidiluter and CVS size distributions suggest that dilution ratio, temperature-related wall interactions, and differences in tunnel background between the diluters contributed to creating nanoparticle concentrations that sometimes exceeded diesel baseline concentrations when driving under load. The results do not support use of CVS dilution methodology for ultrafine particle sampling, and, despite attention to collection of tunnel blanks in this study, results indicate that a protocol needs to be determined and prescribed for taking into account tunnel blank "emissions" to obtain meaningful comparisons between different technologies. Of critical importance is determining how temperature differences between tunnel blank and test cycle sampling compare in terms of background particle numbers. Total particle number concentrations for the minidiluter sampling point were not significantly different for the two alternative technologies when considering all the steady-cycle data collected. Concentrations ranged from 0.8 to 3×10^6 for the baseline bus operating on ultralow sulfur fuel, from 0.5 to 9×10^4 for the diesel bus equipped with the CRT filter, and from 1 to 8×10^4 particles/cc for the CNG bus.

Introduction

Recent regulations address the noxious particulate and gas emissions from heavy-duty diesel engines (*1*−*3*). In urban areas, transit buses are a significant source of heavy-duty vehicle traffic, and many municipalities, including Los Angeles, Sacramento, Cleveland, and Atlanta, have recently modified their fleets to compressed natural gas (CNG) as the "clean" alternative to conventional uncontrolled diesel vehicles to meet increasingly strict particulate matter (PM) air quality regulations. Current PM air quality criteria are mass-based and motivate reducing large diameter PM, but little is known about the ultrafine (diameter < 100 nm) and nanoparticle (<50 nm) emissions from alternative engine technologies. This study was designed to measure the number size distribution of ultrafine and nanoparticles in the exhaust of two in-use "green" technology heavy-duty vehicles (HDV): (1) a spark-ignition compressed natural gas (CNG) certified for operation without an oxidation catalyst and (2) a conventional diesel bus operating on ultralow sulfur fuel (11 ppm S content) with a passive DPF manufactured by Johnson-Matthey and known as a Continuously Regenerating Trap (CRT). For comparison, tests were also conducted on the same diesel vehicle with the DPF replaced by a retrofit-kit catalyzed muffler approved for use by the original equipment manufacturer (OEM). The CNG bus is powered by a diesel engine modified to operate on natural gas.

Many factors highlight recent interest in heavy-duty vehicle PM emissions: (1) diesel vehicle exhaust is listed as a toxic air contaminant by the California Air Resources Board (CARB) and a mobile source air toxic by the U.S. EPA (*4, 5*); (2) recent studies indicate an association between ultrafine and fine particles and human mortality (*6*) and lung tumors in rats (*7*); (3) there is concern that newer heavy-duty vehicle technologies developed to meet *mass* emissions regulations may increase nanoparticle *number* concentrations in vehicle exhaust (*8*−*10*); and (4) fuel composition, known to affect PM emissions, is changing (*11*). Furthermore, concerns have also been raised that particle number concentration or surface area, rather than mass concentration, may have a more direct relationship with adverse human health effects because ultrafine particles are more toxic to lung tissue than fine particles of identical composition (*12*).

No widely accepted test protocol exists for accurately measuring internal combustion engine exhaust particle size distributions under laboratory conditions. A number of significant research efforts are currently addressing the issue of standardization of number emission measurements, but conclusions are likely still some time away because of the complexities involved. Various laboratories, employing dif-

* Corresponding author phone: (860)486-3941; fax: (860)486-2298; e-mail: baholmen@engr.uconn.edu.
† University of Connecticut.
‡ California Environmental Protection Agency.

10.1021/es015884g CCC: $22.00
Published on Web 11/05/2002

ferent dilution techniques and sampling methods, have documented that sampling conditions such as relative humidity, temperature, dilution ratio, and dilution rate can significantly affect measured size distributions and may create nanoparticle artifacts (*13*−*21*). Despite these hurdles, laboratory dynamometer tests continue to be used to compare particle emissions from different types of vehicles because of the benefits of relatively controlled sampling conditions in the laboratory environment.

Recent studies have characterized particle size distributions from diesel and alternative heavy-duty vehicles. Of relevance to the current study are investigations with CNG and CRT engines and vehicles. Studies comparing regulated emissions using a portable dynamometer and CVS dilution tunnel from three alternative fuel (CNG, methanol, ethanol) vehicles (*22*) and from school buses (*23*) showed that CNG vehicles had the lowest total PM mass emissions of all the alternatives tested and were significantly lower than conventional diesel vehicles. The CNG school buses also had higher carbon monoxide (CO) and hydrocarbon (HC) emissions and slightly lower NO_x emissions than the diesel vehicles (*23*). The higher CO and HC emissions from the CNG vehicles are attributed to the lack of use of an exhaust catalyst, a condition that is typical of approved in-use CNG vehicles. For example, CNG buses comprised 70% of the Los Angeles transit bus fleet in November 2001, and 69% of the CNG buses were operating without oxidation catalysts (*24*).

Warren et al. (*25*) originally documented the CRT's ability to reduce not only total particulate mass, the soluble organic fraction (SOF) and gaseous CO and HC from diesel exhaust, but also ultrafine particle number emissions. They reported a 1 order of magnitude reduction in nanoparticle emissions for a Euro II engine equipped with a CRT and operating at constant speed under different loads (*25*). More recently, Lanni et al. (*26*) reported similar findings to that of Warren et al. for New York City transit buses equipped with the CRT and operating at 15 mph and 30 mph. These authors measured particle size distributions with an electrical low-pressure impactor (ELPI) (30−6800 nm) after a 1:100 dilution ratio, one-stage minidilution tunnel (25 °C, 20−30% relative humidity, <0.1 s residence time) and found significant (∼100×) reductions in total particle number concentrations with the CRT filter but no change when the diesel bus was operated on ultralow S fuel (27 ppm S; compared to 247 ppm S diesel fuel) (*26*). Thus, for accumulation mode particles the CRT particle filter reduced diesel vehicle particle emissions more than did the change in fuel S content. In contrast, scanning mobility particle sizer (SMPS) measurements during steady-state cycles showed up to 10× concentration reductions between the low and ultralow S fuel, but only for nanoparticles between ∼7 and 15 nm and only at some vehicle speeds (*26*). The CRT particle filter reduced particle number concentrations over the entire SMPS size range (5−250 nm) by a factor of ∼100. The effect of engine load on ultrafine particle emissions from CNG engines was examined for steady-state engine operation using a single-stage ∼5:1 dilution tunnel (*27*). These authors reported the following: (i) monomodal particle size distributions with count median diameters (CMD) of 20−60 nm for 5 engine loads (35−100%), (ii) maximum 15−700 nm total particle concentrations of $\sim 10^7$ cm^{-3}, and (iii) linear relationships between engine load and both total particle number and CMD (*27*). The small median diameters, monomodal distributions, and abundance of sub-20 nm particles measured by Ristovski et al. was different from an earlier study on light-duty vehicles (*28*). The light-duty CNG and gasoline engines produced smaller particle mean diameters than diesel engines and had total particle numbers (15−700 nm) significantly lower than diesels, and the CNG vehicles had bimodal (modes at ∼60 and 120 nm) distributions at low load (*28*). At high loads, the CNG nanoparticle mode (∼50 nm) approached the total number concentrations seen for a catalyzed diesel engine (*28*).

These few studies highlight the need to examine the ultrafine particle emission potential of alternative heavy-duty vehicle configurations under a range of real-world operating conditions. The present study compares two alternative transit bus technologies, both powered by Detroit Diesel Corporation engines—a compressed natural gas engine operated without an oxidation catalyst and a conventional diesel engine with particle trap after-treatment—in terms of their particle number size distributions over a range of 6−237 nm mobility diameter. The objective of the study was to quantify the ultrafine particle number size distributions under different driving cycle conditions as part of a larger study being conducted by CARB on the relative toxicity of in-use transit bus emissions (*29*). The relationships between particle size distributions collected simultaneously under two dilution conditions are discussed for two steady-state driving conditions: idle and 55 mph cruise.

Experimental Methods

Dynamometer Tests. Chassis dynamometer tests were conducted at CARB's Heavy-Duty Vehicle (HDV) emissions testing laboratory located at the Los Angeles County Metropolitan Transit Authority's (LACMTA) Regional Rebuild Center. A Model 62 Schenck-Pegasus heavy-duty vehicle chassis dynamometer with a single 72-in. diameter roller driven by a direct current 675 hp motor was used for all tests. The laboratory's Horiba critical flow venturi CVS dilution system consists of an 18-in. diameter stainless steel primary dilution tunnel per Code of Federal Regulations (CFR). The dilution air for the CVS tunnel is HEPA-filtered and carbon-treated ambient air. The vehicle exhaust pipes were connected to the inlet of the CVS primary tunnel with a 5 ft long, 6″ (15.24 cm) ID corrugated 316 stainless steel pipe. This transfer line was not insulated. Particle size distribution measurements were made simultaneously using two SMPS instruments (model 3936L25, TSI, Inc.). One set of SMPS measurements was made from a sampling probe installed in a section of the CVS tunnel located 5.3 m downstream of the raw exhaust inlet. This sampling location coincided with the collection point for all gaseous samples to determine regulated and nonregulated gas emissions as well as secondary dilution for collection of total PM mass criteria emissions (*29*). A second SMPS instrument sampled a small portion of the raw exhaust just prior to entering the CVS through a one-stage minidilution system (see Figure 1). This corresponded to the most practical and closest location to the end of the vehicle's exhaust system. The minidilution system consisted of a perforated stainless steel probe located inside the raw exhaust inlet tube (A, Figure 1), a curved 12″ section of $^1/_4$″ stainless steel tubing (B), a nickel foil restricting inlet orifice and orifice meter to measure the sample flow rate (C), a Dekati diluter (Dekati, LTD, Finland) (D), a source of dry (silica gel), hydrocarbon free (activated charcoal) HEPA-filtered compressed ambient temperature air (E), and a 6-foot section of insulated stainless steel 1″ diameter tubing that acted as a residence time chamber (F). The physical constraints and requirements imposed by elevated exhaust pipes of the test vehicles and the lack of space in the laboratory required the use of unusually long sampling trains for delivery of the sample to the instruments. At the outlet of the residence tube, the dilute exhaust was directed to one SMPS and a 30 Lpm Electrical Low Pressure Impactor (ELPI) through conductive silicone tubing. Excess diluted exhaust was directed to a separate laboratory exhaust vent (G). Exhaust and dilution temperatures were recorded using thermocouples located at the point where raw exhaust entered the CVS tunnel (near point A, Figure 1), at the exit of the Dekati

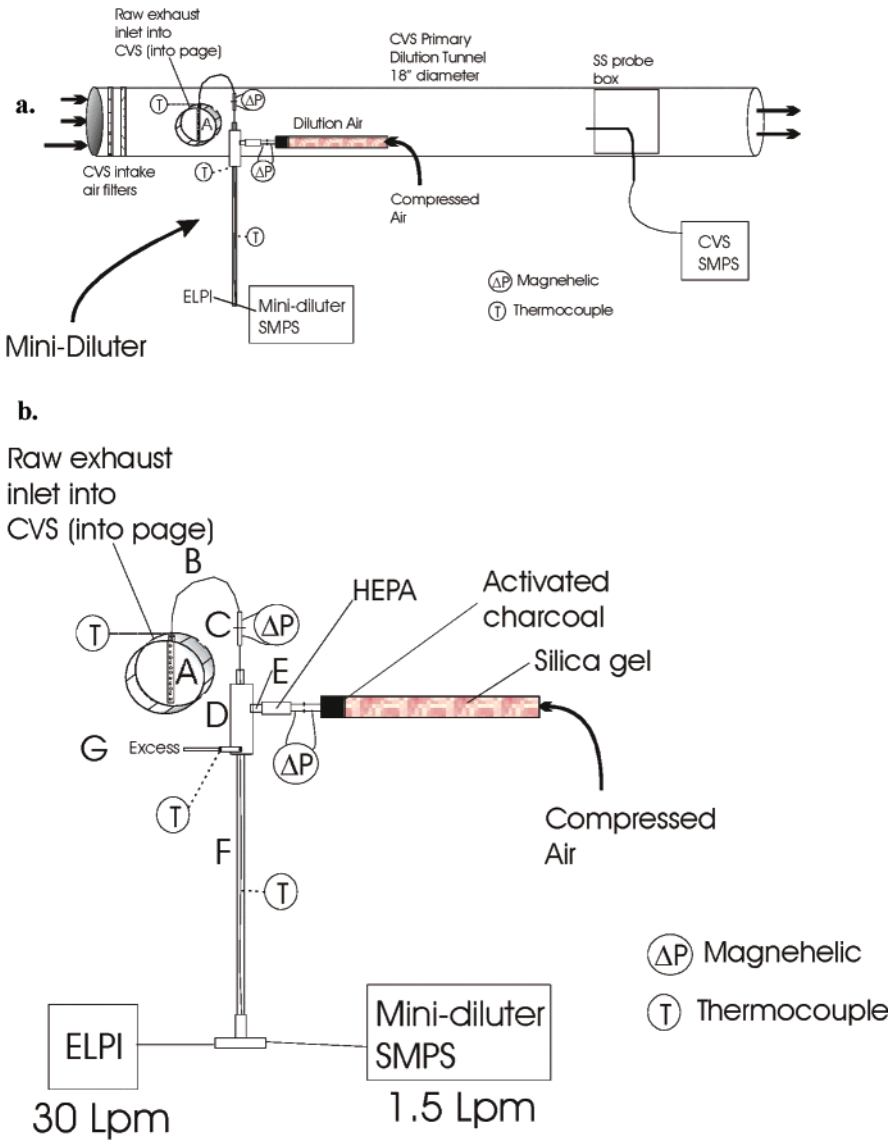

FIGURE 1. Schematic of dilution systems for dynamometer testing: (a) CVS and minidiluter setup relationship shows that SMPS measurements were made simultaneously at the exit of the minidilution tunnel ("minidiluter SMPS") and 5.3 m downstream inside the CVS primary dilution tunnel ("CVS SMPS") and (b) close-up of the minidiluter. Lettered symbols on minidiluter refer to descriptions in the text.

TABLE 1. Transit Bus Vehicles

	natural gas[a] "CNG"	baseline "diesel OEM"	trap diesel "CRT"
fuel:	compressed natural gas	ultralow sulfur ECD-1	ultralow ECD-1 sulfur
MTA bus #:	5300	3007	3007
weight:	33150 lbs	30510 lbs	30510 lbs
model year:	2000	1998	1998
engine model:	50G	EC50	EC50
after-treatment:	none (no oxi. cat.)	OEM catalyzed muffler	DPF Johnson-Matthey continuously regenerating trap (CRT)

[a] The CNG bus was also tested after an additional 500 miles of fleet use ("CNG-retest"). Note that the CNG bus is a modified DDC diesel engine optimized to operate on CNG fuel.

diluter (point G, Figure 1), at the surface of the minidiluter residence tube between the stainless steel tube and its insulation, and at the point of SMPS sampling in the CVS tunnel. Raw exhaust temperature and diluted exhaust temperatures were recorded at approximately 10 Hz and averaged over one second for some test cycles. Recording magnehelics (Dwyer Instruments) were used to record differential pressure across the orifices on the sample and dilution air streams.

Two transit buses recruited from the LACMTA fleet (Table 1) were tested in three different configurations—a CNG without an oxidation catalyst, a diesel with an OEM catalyzed muffler ("OEM") and the same diesel bus with a diesel particulate filter ("CRT"). Both diesel configurations ran on ultralow-sulfur emission control diesel (ECD-1) fuel supplied by ARCO (a BP company). The choice of test buses was determined by the current in-service fleet mix in Los Angeles. The only requirements were (1) "late-model" vehicles and

(2) similar or equivalent engine technology on both CNG and diesel versions. At present, as stated previously, 69% of the CNG buses in the test fleet are operating without oxidation catalysts (*24*). Vehicles were tested on idle and 55 mph steady-state "loaded" cruise at 60% of the vehicle's available power (SS55). For the steady-state cruise tests, the dynamometer gradient was set to achieve ~60% of each vehicle's full power load as determined experimentally by speed-power measurements prior to the driving cycle tests. The 60% load corresponded to dynamometer gradient settings of 0.6% for the CNG bus and 1% gradient for the diesel OEM and CRT vehicles. The CNG bus was retested (CNG-retest) at two gradient settings (0% and 0.6%) on steady-state cycles at the end of two additional months in service. Buses were preconditioned daily prior to the start of all tests by running at 50−55 MPH steady state for at least 15 min. All three vehicle configurations were New Flyer chassis transit buses equipped with Detroit Diesel Model series 50 engines (8.5L, 4 cylinder, 4 stroke). The DPF after-treatment device was a new Johnson-Matthey Continually Regenerating Technology (CRT) particulate filter that was degreened prior to testing. Two drums of BP/ARCO ultralow ECD-1 fuel with a sulfur content of 11 ppm were used for all OEM and CRT diesel testing. All fuel and oil analysis results have been published (*29*) and are provided in the Supporting Information.

Scanning Mobility Particle Sizer (SMPS). Both SMPS instruments were outfitted with TSI model 3081 long DMAs, TSI model 3025A ultrafine CPCs, and AIM software version 4.0. The SMPS instruments were operated at an aerosol flow rate of 1.4 (or 1.45) Lpm, a sheath flow rate of 14 Lpm, and an up-scan time of 120 s (30 s retrace) to give a maximum full scan mobility diameter range of 6−237 nm. All SMPS scans were collected with a logarithmic resolution of 64 channels per decade. Instrument operation was checked daily before and after testing using HEPA filters on the SMPS inlets. In addition, a performance audit of both SMPS instruments was conducted with an electrospray aerosol generator (TSI model 3840) and sucrose aerosol midway through the sampling. The number-weighted size distributions of the two instruments agreed within 10%. This performance audit is one of the recommendations recently made as a quality assurance measure for other relevant diesel aerosol sampling methodology research in the U.S. (*30*).

Dilution Ratio. The minidilution tunnel incorporated two orifice meters with transmitting magnehelics to record second-by-second sample and dilution air flow rates. Labview (National Instruments) running on a laptop computer stored the magnehelic readings. Prior to testing, the magnehelics and orifice meters were calibrated using a BIOS DC-2 Dry Cal flow meter. At the completion of testing, the dilution system was returned to the laboratory fully assembled to generate calibration curves of the orifice meters when positioned within the dilution system. This way, the flows were determined for the actual hardware configuration but under room-temperature conditions. No corrections were made for temperature differences between diluter calibration and sampling conditions.

Average dilution ratios in the CVS tunnel were measured using the ratio of CO_2 concentrations measured in the raw exhaust and in the CVS primary tunnel near the SMPS sampling probe location. Modal CO_2 raw and dilute concentrations were measured in real-time at approximately 1 Hz during individual cycle tests on different vehicles and aligned based on the time stamp and the speed trace record. All CO_2 measurements were background corrected, including humidity.

Residence Times. The approximate exhaust residence time between tailpipe emission and SMPS sampling by the two instruments was calculated using the sampling tube diameters, measured flow rates for the minidilution system, the constant flow rate of the CVS system (2500 scfm), and the measured distance from the CVS inlet to the SMPS sampling probe for the CVS SMPS instrument. The residence time between CVS inlet and the sampling probe located 5.3 m down the CVS tunnel was approximately 0.7 s. Additionally, eight feet of conductive silicone tubing at a SMPS flow rate of 1.4 Lpm gave a total sample train residence time of approximately 5.7 s. The minidiluter residence time depended on which of two sample inlet orifice plates was used. For both dilution ratios the residence time in the six-foot tube of the dilution setup was constant (1.3 s) because of the fixed total flow rate (31.4 Lpm) exiting the Dekati Diluter into the residence tube. For the nominal dilution ratio of 64, the exhaust sample flow rate into the minidiluter was ~0.5 Lpm, and the total sampling train residence time was 5.7 s for the SMPS instrument and 2.2 s for the ELPI. For the nominal dilution ratio of 18, the sample flow rate was ~1.8 Lpm, and the sampling train residence time was 5.3 s for SMPS and 1.8 s for ELPI. Note that for both the CVS and the minidiluter sampling points the 5−6 s overall sampling train exhaust residence times were chiefly determined by the physical constraints in the laboratory where the CVS tunnel is at approximately 15 feet above ground level. Estimates of particle losses in the silicone tubing via diffusion were not considered significant (~3−12% of total particle numbers over SMPS diameter range based on theory). Results were not corrected for losses known to occur in the DMA column (*30*, *31*).

Results

Dilution Ratio. Second-by-second measurements of the minidiluter dilution air and sample flow rates over the sampling periods gave an average dilution ratio of 64 ($\pm$ 5.8, 1 σ) for tests conducted with the 0.0135 in. (0.0343 cm) diameter nickel foil sample inlet orifice. Tests were conducted with this foil for the CNG, diesel OEM, and CRT vehicles. Additional steady-state tests conducted on the CNG-retest vehicle employed a larger sample inlet orifice (0.028 in. (0.071 cm) diameter), and the resulting nominal dilution ratio was 18. The average dilution ratios in the CVS tunnel were estimated to be approximately 35 and 8 for the IDLE and steady-state 55 mph (SS55) cycles, respectively. All SMPS data presented here, with the exception of the tunnel blanks, are corrected for the tunnel background and dilution ratio.

Comparisons of Vehicles by Cycle. *Tunnel Blanks.* Tunnel blanks (TB) were used to assess "background" particulate matter levels in the CVS tunnel and minidiluter sampling train (Figure 2). TB counts were generally low (i.e., $<10^3$ cm^{-3} in each size bin), and TB concentrations were lower than those measured for the ambient air in the laboratory test bay. Tunnel blank concentrations were lowest during the diesel OEM and CNG-retest bus sampling (Figure 2). During the CRT bus CVS tunnel blank runs, significantly more nanoparticles in the <20 nm diameter range were measured than for the CNG or OEM vehicles. These differences are likely due to release of stored material deposited in the dilution tunnel during other vehicle testing conducted during this study, but this issue was not investigated further due to time constraints. A number of researchers have described a memory effect or have observed a storage-and-release effect in various sampling approaches, and this is believed to have played a role in this study (*32*). Further, the potential for artifacts originating from hydrocarbon material stored in the transfer hose connecting the tailpipe to the dilution tunnel and coagulation, condensation, and chemical changes that occur during exhaust transport have been documented (*32*, *33*). These previous observations prompted the rigorous monitoring and collection of TB samples in this study in order to quantify the role of the TB and its impact on measured emissions because the emissions testing facility

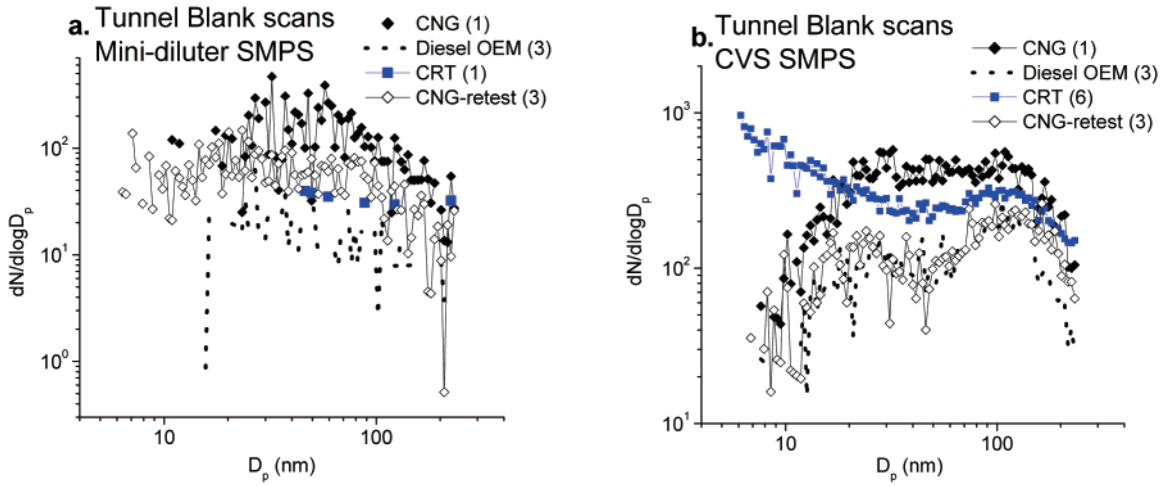

FIGURE 2. Average tunnel blank 6−237 nm particle size distributions collected by (a) the minidiluter SMPS and (b) the CVS SMPS during testing of vehicles listed in legend. Note that the *y*-axis scales are different. Numbers in legend are number of tunnel blank tests averaged for that bus.

TABLE 2. Mean Thermocouple Temperatures (°F) and Test Bay Dewpoint[a]

		bay ambient		bay dewpoint		raw exhaust		minidiluter		CVS box		number
cycle	bus	mean	s.d.	mean	s.d.	mean	s.d.	mean	s.d.	mean	s.d.	n
idle	CNG	72.5	0.3	50.0	1.3	291.3	3.3	73.5	0.4	70.4	0.2	4239
	CNG	72.0	0.1	50.2	1.4	288.7	0.7	71.8	0.0	70.4	0.4	4239
	CRT	82.9	0.2	58.3	2.2	206.2	0.5	86.0	0.2	nd	nd	4239
	CRT	84.7	0.3	57.6	2.1	205.9	0.7	85.7	0.2	nd	nd	4239
	diesel OEM	*79.4*	*0.1*	*41.5*	*1.0*	*165.4*	*0.2*	*83.3*	*0.1*	*nd*	*nd*	*2119*
steady-state at 55 mph	CNG	*75.1*	*2.4*	*49.5*	*1.4*	*827.4*	*15.6*	*82.7*	*3.9*	*93.2*	*12.4*	*4240*
	CNG	*75.0*	*3.3*	*48.5*	*1.2*	*818.3*	*27.4*	*82.5*	*2.7*	*95.7*	*11.1*	*4240*
	CNG-retest	*70.4*	*0.7*	*56.5*	*1.7*	*844.6*	*4.6*	*101.6*	*2.0*	*78.0*	*2.4*	*1145*
	CNG-retest	*73.2*	*1.6*	*56.6*	*1.8*	*870.0*	*7.0*	*103.8*	*1.7*	*78.1*	*3.4*	*1159*
	CRT	73.7	0.7	45.7	1.8	694.5	5.9	89.3	3.1	nd	nd	4238
	CRT	78.7	0.6	39.3	1.5	700.1	4.2	90.8	1.6	nd	nd	4238
	CRT	*82.6*	*1.6*	*36.9*	*1.6*	*697.9*	*8.4*	*90.5*	*0.7*	*nd*	*nd*	*4239*
	CRT	*85.7*	*0.8*	*33.2*	*2.0*	*705.5*	*2.5*	*90.9*	*2.0*	*nd*	*nd*	*4238*
	diesel OEM	71.7	1.1	50.9	1.2	662.1	8.8	84.6	2.9	nd	nd	4247
tunnel blank	CNG	70.1	0.5	48.6	1.3	120.9	3.2	71.8	0.4	68.8	0.2	4239
	CNG	69.3	0.3	49.1	1.1	108.8	1.8	70.0	0.2	67.3	0.2	4239
	CNG-retest	72.9	0.4	55.0	1.4	75.9	0.5	96.3	0.5	74.2	0.1	2119
	CNG-retest	73.0	0.3	54.9	1.4	73.6	0.3	71.3	0.4	73.5	0.1	2119
	CRT	81.4	0.4	35.1	2.2	81.1	0.7	89.7	0.8	nd	nd	4239
	CRT	80.9	0.5	34.8	2.0	80.3	0.5	87.8	0.3	nd	nd	4239
	CRT	84.4	0.2	57.6	2.2	83.0	0.2	87.7	0.1	nd	nd	4232
	diesel OEM	68.0	0.3	49.3	1.2	69.3	0.2	75.2	0.2	nd	nd	2119

[a] Italicized entries correspond to tests that had distinct nuclei modes. Ambient air temperature and dewpoint were measured in the dynamometer bay. Number is number of thermocouple readings averaged.

was not dedicated solely to the present project. Chronologically, a school bus equipped with a soot trap was tested prior to testing of the first vehicle (CNG bus) in this project. After the CNG testing, a Class 8 truck was tested, followed by the diesel OEM and CRT vehicles. A school bus was tested after the CRT followed by the CNG-retest to conclude the present study. All data reported here are corrected for the average of all tunnel blanks collected during a given vehicle's tests. Each tunnel blank test was approximately 35 min in length. It should be recognized that direct subtraction of tunnel blank distributions from the vehicle test data is not straightforward due to large differences in sample air temperature during blank and test cycle sampling, as discussed in more detail below (see Table 2). Nevertheless, lacking comprehensive data on how temperature affected background particle concentrations during this study, the significant differences in measured tunnel background distributions, especially under CVS sampling conditions (Figure 2), necessitated background correction on a vehicle-by-vehicle basis in order to facilitate comparisons between the different bus configurations. The degree to which the vehicle test results are determined by the subtraction of different tunnel backgrounds will depend on the relative blank vs test period emission levels and needs to be studied further, especially as heavy-duty vehicle PM emission limits are reduced in the future.

Minidiluter blanks were lower than CVS tunnel blanks, likely due to the fact that this system had higher dilution ratios and was not used during the testing of other vehicles.

Idle Operation. As expected, the diesel OEM (i.e., diesel baseline) bus had the highest IDLE cycle particle counts and also showed a distinct bimodal distribution under both the CVS and minidiluter conditions (Figure 3). The diesel OEM number emissions were generally 1−2 orders of magnitude higher than emissions from either of the alternative buses. The CNG bus did not have a bimodal distribution during IDLE tests, and the CRT bus bimodal distribution was evident only on the CVS tunnel distribution (Figure 3b). The

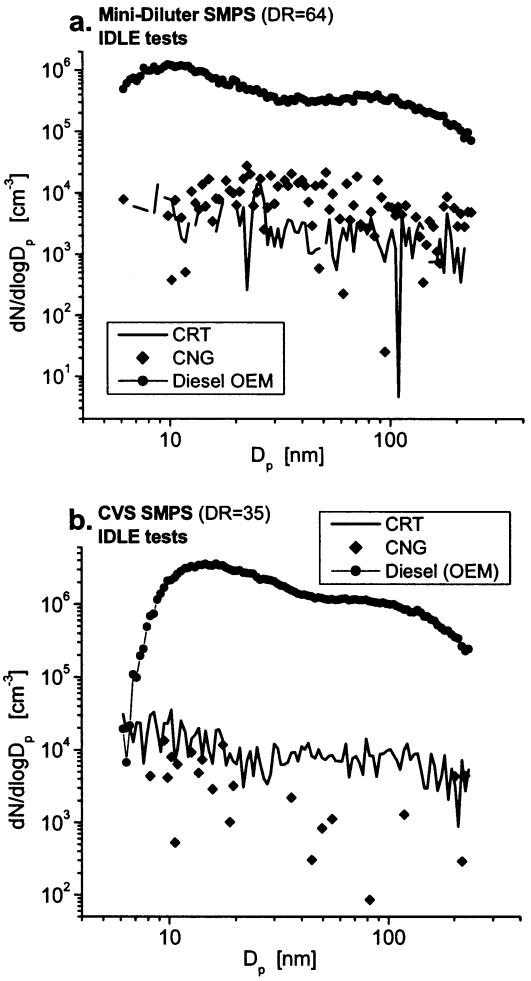

FIGURE 3. SMPS full scan average results for IDLE tests: (a) SMPS sampling from minidilution system (dilution ratio, DR = 64) and (b) SMPS sampling from CVS tunnel (DR = 35). Note that the *y*-axis scales are different.

accumulation mode distribution for the diesel bus with and without the diesel particulate filter covered the same diameter range (approximately 30−200 nm; see Figure 3b), but particle concentrations were 2 orders of magnitude smaller for the CRT bus compared to the diesel OEM. The low IDLE cycle concentrations resulted in relatively noisy SMPS distributions for both the CNG and the CRT buses compared to diesel OEM on both diluters (Figure 3). The relative number concentrations for the CNG and CRT buses during IDLE differed between the two dilution systems. For the minidiluter, the CNG counts exceeded those measured for the CRT bus over most of the SMPS sample range (6−237 nm) by up to a factor of 10 (Figure 3a). Under CVS dilution conditions, however, the CRT emissions exceeded those measured for the CNG bus by up to a factor of 100 (Figure 3b, note that missing values mean IDLE counts were less than tunnel blank). This difference between dilution systems may partly be explained by differences in the CVS tunnel blanks between the buses (Figure 2b) because the CNG bus IDLE cycle counts were lower than the relatively high CVS tunnel blank during CNG bus testing. During CRT testing, the tunnel blank counts were about half those measured during the IDLE cycle. These data highlight the importance of collecting sampling train background particle number concentration data in order to obtain meaningful comparisons between different vehicle technologies. Furthermore, it is significant that the vehicle without the oxidation catalyst (CNG) did not have significantly higher nuclei mode particle

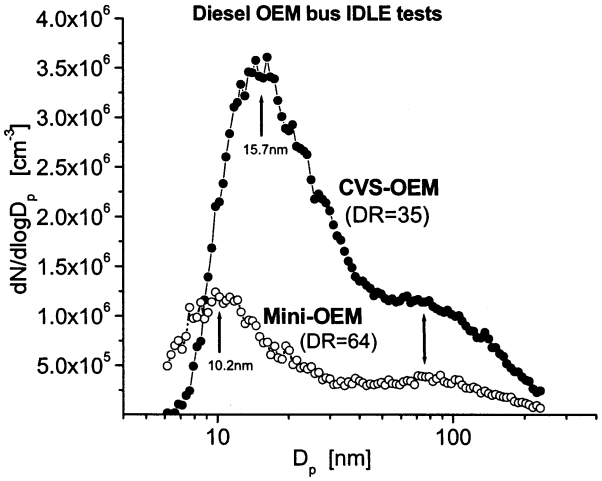

FIGURE 4. Average IDLE cycle size distributions for baseline diesel OEM bus plotted with linear *y*-axis scale indicate differences in nuclei mode under two dilution conditions.

concentrations than the other buses, despite having as large an organic carbon to elemental carbon ratio in the total PM measurement (*34*, *35*). The average composition of the measured PM for the vehicle configurations tested as a function of duty cycle is provided in the Supporting Information.

During IDLE, the diesel OEM bus released relatively more volatile precursors per amount of carbonaceous material combusted relative to driving under load as evidenced by the organic carbon to elemental carbon ratio (*34*, *35*). The volatile precursors nucleate upon rapid dilution in both diluters and result in distinct nuclei-modes in both number-weighted size distributions (Figures 3 and 4). Comparison of the IDLE particle number distributions for the diesel OEM bus configuration between the two dilution systems indicates the possibility that particle precursors were lost to or that nanoparticle growth occurred in the CVS dilution tunnel (Figures 3 and 4). Growth of nanoparticles in the CVS tunnel is suggested by (i) the disappearance of particles at diameters <10 nm only at the CVS sampling point (compare parts a and b of Figure 3; see Figure 4); (ii) the broadening of the diesel OEM IDLE distribution nuclei mode on the CVS SMPS relative to the minidiluter (Figure 4, note that minimum between modes shifted from 32 nm at minidiluter to 52 nm at CVS); and (iii) the shift in the nuclei peak from 10 nm at the minidiluter to ∼15 nm at the CVS sampler (Figure 4). Careful examination of published ultrafine size distributions from a medium-duty diesel engine operating at steady-state show a similar broadening and shift of the nuclei mode collected using a minidilution system, but only at high dilution system residence times (e.g., 1000 ms; compare Figures 2 vs 6 vs 9 and Figures 3 vs 7 vs 10 in ref *14*). Because the computed exhaust particle residence times for the CVS and minidiluter sampling points were both ∼6 s, dilution residence time cannot explain the observed difference between the size distributions on the two diluters. It is more likely that differences in overall dilution ratio between the two sampling systems played a significant role in the nanoparticle growth process. Note that the accumulation mode (∼70−80 nm) did not shift with dilution conditions (Figure 4). The CVS tunnel IDLE cycle dilution ratio (∼35) was 1.8 times smaller than that for the minidiluter (∼64), and particle growth rate has been observed to decrease with increased dilution ratio (*36*). Thus, growth of the smallest emitted exhaust particles due to adsorption of semivolatile hydrocarbon species would be expected to be faster in the CVS tunnel compared to the minidiluter. Khalek et al. observed ∼45% higher growth rate of freshly nucleated

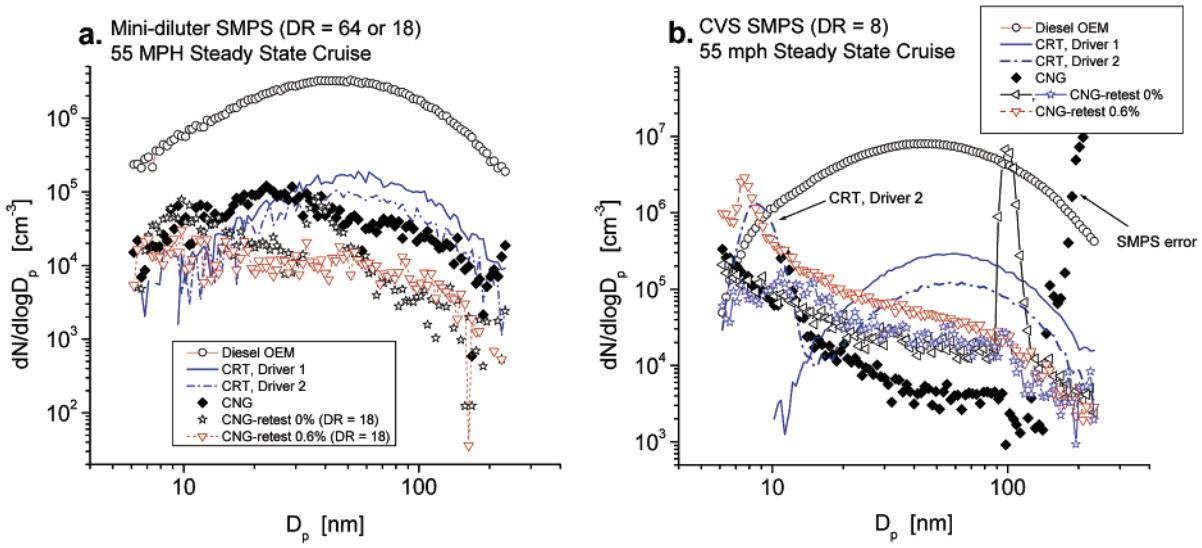

FIGURE 5. Steady-state (55 mph; 60% load) average 6−237 nm SMPS scans for all vehicles: (a) minidiluter SMPS and (b) SMPS sampling from the constant volume sampler (CVS). Note that the *y*-axis scales are different, a lower minidiluter dilution ratio (DR = 18) was used for the CNG-retest bus testing, and SS55 cycle emissions were measured at two different dynamometer gradient settings (0% and 0.6%) for the CNG-retest bus only. The diesel vehicles (OEM and CRT) were measured at 1% gradient and CNG at 0% during SS55 testing to achieve 60% of maximum power for all vehicles.

particles when the dilution ratio was decreased from 40 to 25 (*36*). The diesel OEM nanoparticle growth rates can be estimated from the measured nuclei mode peaks in Figure 4 and the dilution tunnel residence times. Assuming 1 nm nuclei initially and 5.7 s residence times for both dilution systems as stated above, the CVS and minidiluter growth rates are 2.6 and 1.8 nm/s, respectively. These rates are similar to the smallest rates observed by Khalek et al. and are surprisingly low considering that operation on ultralow sulfur fuel is expected to enhance nanoparticle growth rate (*36*). Other processes such as outgassing of contamination on the walls of the CVS tunnel may have also enhanced particle growth in the CVS tunnel relative to the minidiluter. Detailed investigation of this issue is beyond the scope of the present study, but further systematic study of the effects of temperature, humidity, dilution ratio, and residence time on nanoparticle formation and growth are clearly needed to identify the most appropriate methodology for characterizing particle size distributions in vehicle exhaust, especially for vehicle operation on reduced S diesel fuel that will be mandated for use by June 2006 (*1*).

Steady-State Cruise. The diesel OEM bus steady-state cruise cycle (SS55) size distribution was broad and monomodal (mode ∼40−60 nm) at the minidiluter (Figure 5a) and a broad mode with a small shoulder at 10 nm was observed in the CVS tunnel (Figure 5b). These accumulation mode diameters were smaller than those measured for IDLE cycles (70−80 nm). Under SS55 operation, the engine in the diesel OEM bus was subjected to high-speed and medium-load. The release of carbonaceous soot material under these conditions (5−10× higher than under IDLE cycle; compare accumulation mode in Figures 3 and 5) appears to be sufficient to adsorb the volatile precursors for nuclei-mode particles and suppress nucleation. In the CVS relative to the minidiluter, the 8× lower dilution ratio would tend to promote nanoparticle formation and this may explain the shoulder in the CVS SMPS data at 10 nm (Figure 5b).

On the 55 mph steady-state cruise cycle (SS55), under some sampling conditions, both the CNG and CRT vehicles displayed large (<10 nm) nuclei modes and particle concentrations that approached or exceeded those from the diesel OEM bus (Figure 5). The minidiluter SMPS size distributions for both CNG and CRT were more consistent both between buses and between test cycle repetitions on a single bus than were the distributions measured at the CVS tunnel (Figure 5). The shapes of the CRT and diesel OEM size distributions were similar at the minidiluter and engine load (e.g., dynamometer gradient setting 0% or 0.6%) appeared to have no significant effect on the CNG bus emissions during steady-state operation (Figure 5a). The SS55 minidiluter data also show that the CNG vehicle consistently emitted higher (<20 nm) nanoparticle concentrations than the CRT vehicle, whereas the CRT bus emitted higher concentrations than the CNG for particles larger than ∼30 nm (Figure 5a).

The variability in size distributions measured under CVS sampling conditions for a single bus are indicated by the SS55-CRT bus data where two different drivers had significantly different size distributions (Figure 5b), but the distributions were similar at the minidiluter location (Figure 5a). Each driver ran two SS55 cycles, and the individual cycles were separated by periods of idle and at least 15 min of warm-up. The fact that CRT bus emissions for Driver 1 had no nuclei mode at the CVS sampling location, but Driver 2 had concentrations exceeding those of the diesel OEM, indicates that CVS dilution processes alone did not generate the observed nuclei mode. The effects of driving style on regulated emissions have already been discussed in the literature (*37*, *38*); a driver effect on particle number emissions is also possible. Thus, changes in engine operating parameters, the trapping efficiency of the CRT, and diluter properties likely played a role in nanoparticle formation under the moderate CVS dilution conditions and the lower concentration of accumulation mode particles observed for the CRT bus relative to the diesel OEM.

The SMPS scans at the CVS location showed extremely high counts at large diameters for some SS55 tests with the CNG bus (i.e., Figure 5b, CNG). The large counts at ∼200 nm measured during the CNG tests (not the CNG-retest) were registered during a CPC saturator high-temperature error on the CVS SMPS on repeated scans during the SS55 cycle. The high-temperature error occurs at temperatures >40 °C and was seen only for the CNG bus SS55 tests likely due to its significantly higher exhaust temperature when operated under load (see Table 2). These data are included in Figure 5b to show that despite the SMPS error at high DMA voltage settings, the counts recorded at lower voltages (smaller

TABLE 3. Total SMPS Particle Number Concentrations (#/cm^3) for SMPS 6−237 nm Scans

		IDLE		steady-state cruise	
bus		minidiluter	CVS	minidiluter	CVS
diesel	mean	8.00E+05	2.42E+06	2.58E+06	6.19E+06
OEM	sd	2.24E+04	9.16E+04	7.22E+04	4.89E+05
CRT	mean	5.12E+03	1.66E+04	8.54E+04	2.17E+05
	sd	1.43E+02	6.27E+02	2.39E+03	1.72E+04
CNG	mean	1.02E+04	*a*	6.89E+04	1.30E+06
	sd	2.85E+02	1.29E+02	1.93E+03	1.03E+05
CNG-	mean	no data	no data	8.48E+04	5.58E+06
retest	sd	no data	no data	2.37E+03	4.41E+05

[a] Test total number concentration was below Tunnel Blank.

diameters) agreed with the SS55 tests collected during the CNG-retest sampling that did not have an SMPS temperature error. Note that only the CVS SMPS scans displayed the >100 nm peaks; the higher dilution ratio of the minidiluter apparently maintained cooler temperatures that were always within the SMPS sampling range. Temperature differences could explain why the CNG, but not the CNG-retest steady-state cycle, resulted in SMPS errors at the CVS sampling location. During the CNG-retest runs, ambient air temperatures were ∼3 °F cooler and measured CVS dilution air temperatures were ∼10 °F cooler near the SMPS sampling point compared to the CNG tests (Table 2). The data in Table 2 document that raw exhaust temperatures were ∼500 °F hotter during SS55 compared to IDLE cycle tests for all vehicles.

Total Particle Number Concentrations. Average total particle number concentrations between 6 and 237 nm for each vehicle-cycle configuration show generally consistent results between the two dilution systems (Table 3). Higher total particle number concentrations were measured at the CVS tunnel compared to the minidiluter for all bus-cycle pairs except CNG-IDLE where the CVS total number concentration was less than zero after subtraction of the tunnel blank. For the two diesel bus configurations, the ratio of CVS to minidiluter total particle concentrations was a factor of 3 for both the IDLE and SS55 cycles. In contrast, much higher ratios were obtained for CNG and CNG-retest: total particle numbers for SS55 were 19 and 66 times higher under CVS dilution, respectively.

Among the buses, the CRT bus had the lowest total number concentration for the SS55 cycle in the CVS tunnel, but in the minidiluter the CNG and CRT total concentrations were similar and 30 times lower than the diesel OEM bus. The CNG bus had the lowest average number concentration for IDLE at the CVS sampling point because concentrations were similar to those measured for the tunnel blank. In the minidiluter, however, the CRT had the lowest IDLE cycle total concentrations. These results document the 10−100 time reductions in total ultrafine particle number that can be achieved, on average, by using alternative vehicle configurations, as has been previously reported under different dilution systems (*22*, *23*, *26*).

Discussion

Nanoparticle Mode and Exhaust Temperature. Maricq and co-workers (*15*, *32*, *33*) have discussed the nanoparticle artifacts associated with release of material stored on transfer line walls under conditions of high exhaust temperature. If such a mechanism was operating during the present tests, there should be a measurable relationship between raw exhaust temperature and the presence of nanoparticles, particularly at the CVS sampling station. In other words, tests that displayed high nanoparticle mode counts should have had corresponding high exhaust temperatures and tests for the same vehicle that had low nanoparticle concentrations should have had lower measured exhaust temperatures. This analysis assumes that only temperature effects, not driving cycle, contributed to the formation of nanoparticles. The data in Table 2 generally do *not* support this hypothesis. While there were some tests where high temperatures corresponded to the presence of nuclei modes in the distributions, there were also many cases where exhaust temperatures were high, but the nuclei mode was not observed. Thus, the observed nanoparticles are not solely the result of a cool storage and release upon heating of the CVS tunnel walls. However, the CVS tunnel blanks do not account for all of the potential background effects because they were conducted at ambient, not exhaust, temperatures. Another possible explanation is ambient relative humidity since high relative humidity has been shown to lead to nanoparticle formation in diesel vehicle exhaust (*18*, *36*). Relative humidity (RH) was controlled for the minidiluter because dilution air was dried prior to mixing with the exhaust, but the air entering the CVS tunnel was only filtered and not dried. The relative humidity of the ambient air used for CVS dilution was calculated from the measured test bay ambient temperature and dewpoint. As observed for raw exhaust temperature, relative humidity was also not a reliable predictor of nanoparticle formation in the CVS tunnel.

Comparison of Dilution Methods. For the CNG and CRT vehicles, accumulation mode number concentrations were consistently 20−100 times lower than the diesel OEM under both dilution conditions and for both the IDLE and SS55 cycles, with the difference being greater for the CNG bus when operating under load (Figure 6). For the nuclei mode particles, however, distinct differences were observed between the two dilution systems. The CNG bus size distributions often had large nuclei mode particle concentrations, whereas the CRT bus sometimes had significant nuclei mode emissions.

Only at the CVS sampling location did SS55 cycle nanoparticle counts from the alternative vehicles meet or exceed particle number concentrations measured for the diesel OEM bus. In the case of the CNG, the high nuclei mode concentrations may be a result of low emission of carbonaceous soot material (see Figures 5 and 6) combined with release of significant volatile precursors from the lubricating oil and lack of an oxidation catalyst. Nucleation of sulfuric acid/water derived from sulfur in lubrication oil has been proposed as a plausible mechanism for nanoparticle formation when fuel sulfur contents are low (*14*, *36*, *39*) such as it was for the CNG bus (2−5 ppm S) (*29*). The S content in the CNG bus lubrication oil (5400 ppm) was 1.4× higher than that for the diesel bus (3800 ppm) (*29*) and would increase the potential for H_2SO_4/H_2O nucleation in the CNG bus relative to the CRT bus. However, raw exhaust temperatures during SS55 were significantly higher for the CNG bus (850 °F) compared to the CRT and diesel OEM (650−700 °F) (Table 2) and would tend to suppress nucleation because saturation vapor pressures increase with temperature. Without more information on the composition of the nuclei mode particles for the different vehicle types, more detailed discussion concerning nanoparticle formation processes is unwarranted. What is clear from the data is that high dilution ratios (minidiluter) can suppress significant nanoparticle formation (compare parts a and b in Figure 5), but low dilution ratios and high exhaust temperatures for CNG vehicle operation under SS55 load (CVS tunnel data) created conditions for nanoparticle formation and/or possible CVS tunnel outgassing that would likely not be observed under real-world, higher dilution conditions. Thus, while not conclusive, the minidiluter was an unlikely source of nanoparticle artifacts during the testing. It is also possible that the differences in the composition of PM for the CNG and

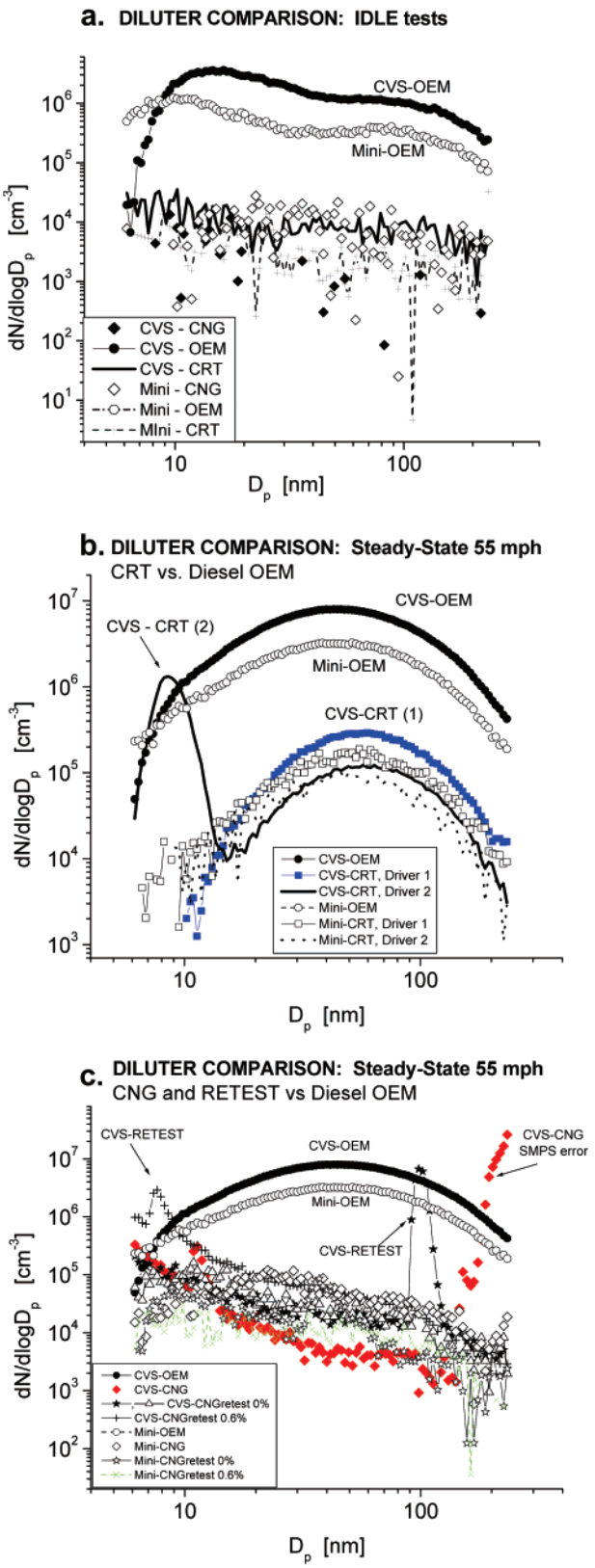

FIGURE 6. SMPS data for both dilution systems (CVS and minidiluter) plotted by driving cycle: (a) IDLE and (b and c) the steady-state cycle data is presented on two plots with the diesel OEM data reproduced to facilitate comparison among numerous distributions. Note that the *y*-axis scales are different on each panel.

diesel vehicles played a role, especially when considering the shift in the balance between volatile particle precursors and the presence of soot in the context of the nonlinearities of the nucleation process. Very few previous studies have examined nanoparticle formation processes for vehicles operating on ultralow sulfur diesel fuel and compressed natural gas. For these vehicles, the source of the nanoparticles may best be inferred from detailed analysis of the composition of the nanoparticle mode, a challenging but important task given that the composition of nuclei mode particles and therefore their toxicity may vary with engine and after-treatment technology. The absence of an oxidation catalyst on the CNG bus may explain why significantly more < 20 nm particles were consistently measured for the CNG and CNG-retest steady-state cruise tests than for the CRT bus at the minidiluter SMPS (Figure 5a). However, if semivolatile hydrocarbon species derived from oil are responsible for the CNG nanoparticle mode, it is not clear that a CNG oxidation catalyst will reduce the nanoparticle number concentration because the primary role of CNG oxidation catalysts is to control low molecular weight volatile organic compounds, especially formaldehyde. Ultrafine particle emissions from oxidation catalyst-equipped CNG buses must be compared to the CNG and CNG-retest data presented here (for a vehicle without an oxidation catalyst) to examine this issue further.

The applicability of these results to real-world dilution must be examined critically. Kittelson and co-workers have reported real-world dilution ratios of 1000:1 and dilution times of ~2 s (*13*, *40*), conditions that were not achieved in the present study. Furthermore, measurement of nanoparticle modes in roadside samples is quite common (*41*−*44*). The lack of a nuclei mode in the diesel OEM bus SS55 distributions measured here likely reflects the use of ultralow sulfur fuel. As this fuel becomes widely used nationwide due to new EPA regulations (*1*), nanoparticle mode emissions from diesel vehicles should generally decrease. However, as the CNG and CRT data here indicate, use of alternative fuels and vehicles (CNG and trap-equipped diesel) may sometimes result in elevated nanoparticle emissions comparable to those of the diesel vehicle.

The implications of the present study for urban areas are that new alternative transit bus engine technologies still represent a significant source of ultrafine particles, albeit at total number concentrations that are 10−100 fold smaller than diesel vehicles running on ultralow sulfur fuel, itself a considerable improvement over conventional diesel fuel operation. Differences in size distributions for bus exhaust measured simultaneously under CVS and minidiluter conditions highlight the fact that extensive work remains to be done to develop a robust emissions sampling protocol for ultrafine particles. Challenging questions pertinent to this choice of sampling methodology should consider whether mitigation of exposure to ultrafine particles should focus on control of particle number or particle surface area. Finally, ultrafine particle emissions from alternative vehicles must be weighed against emissions of gas-phase pollutants such as NO_2 (for CRT) or HCHO (for CNG) in order to assess overall improvements on air quality and human health.

Acknowledgments

The authors thank Harvey Porter, Keith Stiglitz, and Fred Gonzales (CAVTC) for their patience, expertise in dynamometer operation and assistance with setting up the minidilution system; Teresa James, Mark van deWater, and Kathy Nanzetta at UC Davis for help with the minidilution tunnel and datalogger; and Sandeep Mehta (W. Virginia U) for helpful discussions and electrospray measurements. Funding for this study was provided by the California Air Resources Board, the South Coast Air Quality Management District, and NSF BES-0132759. The statements and opinions expressed in this paper are solely the authors and do not represent the official position of the California Air Resources Board. The mention of trade names, products, and organi-

zations does not constitute endorsement or recommendation for use. The Air Resources Board is a department of the California Environmental Protection Agency. ARB's mission is to promote and protect public health, welfare, and ecological resources through effective reduction of air pollutants while recognizing and considering effects on the economy. The ARB oversees all air pollution control efforts in California to attain and maintain health-based air quality standards.

Supporting Information Available

Additional information on the fuel and oil chemical compositions as well as elemental and organic carbon in total particulate matter collected following CFR procedures. This information is available free of charge via the Internet at http://pubs.acs.org.

Literature Cited

(1) U.S. E.P.A. *Proposed heavy-duty engine and vehicle standards and highway diesel fuel sulfur control requirements*; Office of Transportation and Air Quality, 2000.
(2) CARB *California Air Resources Board News Release 99-36* **1999**, 1−2.
(3) CARB *California Air Resources Board News Release 01-11* **2001**, 1−2.
(4) CARB *California Air Resources Board Resolution 98-35* **1998**.
(5) U.S. E.P.A. *Code of Federal Regulations* **2001**, *40 CFR Part 80*, 17230−17273.
(6) Wichmann, H. E.; Spix, C.; Tuch, T.; Wolke, G.; Peters, A.; Heinrich, J.; Kreyling, W. G.; Heyder, J. *Daily mortality and fine and ultrafine particles in Erfurt, Germany, Part I: Role of particle number and particle mass*; Health Effects Institute Research Report 98., 2000.
(7) Stober, W.; Mauderly, J. L. *Inhalation Toxicol.* **1994**, *6*, 427−457.
(8) Bagley, S. T.; Baumgard, K. J.; Gratz, L. D.; Johnson, J. J.; Leddy, D. G. *Characterization of fuel and aftertreatment device effects on diesel emissions*; Health Effects Institute: 1996.
(9) Abdul-Khalek, I. S.; Kittelson, D. B.; Graskow, B. R.; Wei, Q.; Brear, F. *SAE Technical Paper 980525* **1998**.
(10) Johnson, J. H.; Baumgard, K. J. *SAE Technical Paper 960131* **1996**.
(11) Ahlvik, P.; Ntziachristos, L.; Keskinen, J.; Virtanen, A. *SAE Technical Paper 980410* **1998**, 1−20.
(12) Donaldson, K.; Li, X. Y.; MacNee, W. *J. Aerosol Sci.* **1998**, *29*, 553−560.
(13) Dolan, D. F.; Kittelson, D. B. *SAE Technical Paper 790492* **1979**.
(14) Abdul-Khalek, I. S.; Kittelson, D. B.; Brear, F. *SAE Technical Paper* **1999**, *1999-01-1142*, 1−9.
(15) Maricq, M. M.; Chase, R. E.; Podsiadlik, D. H.; Vogt, R. *SAE Technical Paper 1999-01-1461* **1999**, 1−12.
(16) Pagan, J. *SAE Technical Paper* **1999**, *1999-01-1141*, 1−7.
(17) Kittelson, D. B. *J. Aerosol Sci.* **1998**, *29*, 575−588.
(18) Shi, J. P.; Harrison, R. M. *Environ. Sci. Technol.* **1999**, *33*, 3730−3736.
(19) Shi, J. P.; Mark, D.; Harrison, R. M. *Environ. Sci. Technol.* **2000**, *34*, 748−755.
(20) Shi, J. P.; Harrison, R. M.; Brear, F. *Sci. Total Environ.* **1999**, *235*, 305−317.
(21) Collings, N.; Graskow, B. R. *Philos. Trans. R. Soc. London A* **2000**, *358*, 2611−2623.
(22) Wang, W. G.; Clark, N. N.; Lyons, D. W.; Yang, R. M.; Gautam, M.; Bata, R. M.; Loth, J. L. *Environ. Sci. Technol.* **1997**, *31*, 3132−3137.
(23) Clark, N. N.; Gautam, M.; Wang, W.; Boyce, J. A.; Lyons, D. W. *Spring Technical Conference* **1999**, *ICE-32-2*, 17−24.
(24) LACMTA, Customer Relations.
(25) Warren, J. P.; Allansson, R.; Hawer, P. N.; Wilkins, A. J. J. *IMechE S491/006/98* **1998**, 45−55.
(26) Lanni, T.; Chatterjee, S.; Conway, R.; Windawi, H.; Rosenblatt, D.; Bush, C.; Lowell, D.; Evans, J.; McLean, R. *SAE Technical Paper* **2001**, *2001-01-0511*.
(27) Ristovski, Z. D.; Morawska, L.; Hitchins, J.; Thomas, S.; Greenaway, C.; Gilbert, D. *J. Aerosol Sci.* **2000**, *31*, 403−413.
(28) Greenwood, S. J.; Coxon, J. E.; Biddulph, T.; Bennett, J. *SAE Technical Paper* **1996**, *961085*, 105−111.
(29) Ayala, A.; Kado, N. Y.; Okamoto, R. A.; Holmén, B. A.; Kuzmicky, P. A.; Kobayashi, R.; Stiglitz, K. E. *SAE Technical Paper* **2002**, *2002-01-1722*, 1−12.
(30) Ayala, A.; Olson, B.; Cantrell, B. *Working Quality Assurance Project Plan for Diesel Aerosol Sampling Methodology (CRC Project E-43)*; Final Report for Coordinating Research Council, Inc., 2002.
(31) Fissan, H.; Hummes, D.; Stratmann, F.; Büscher, P.; Neumann, S.; Pui, D. Y. H.; Chen, D.-R. *Aerosol Sci. Technol.* **1996**, *24*, 1−13.
(32) Maricq, M. M.; Chase, R. E.; Xu, N. *J. Air Waste Manage. Assoc.* **2001**, *51*, 1529−1537.
(33) Maricq, M. M.; Podsiadlik, D. H.; Chase, R. E. *Environ. Sci. Technol.* **1999**, *33*, 1618−1626.
(34) Okamoto, R. A.; Ayala, A.; Kado, N. Y.; Kuzmicky, P. A.; Kobayashi, R. *Environ. Sci. Technol.* **2002**, in preparation.
(35) Ayala, A.; Kado, N.; Okamoto, R.; Rieger, P.; Holmén, B.; Stiglitz, K. E. *12th CRC On-road Vehicle Emissions Workshop* 2002.
(36) Khalek, I. A.; Kittelson, D. B.; Brear, F. *SAE Technical Paper* **2000**, *2000-01-0515*, 1−9.
(37) Clark, N. N.; Gautam, M.; Rapp, B. L.; Lyons, D. W.; Grabowski, M. S.; McCormick, R. L.; Alleman, T. L.; Norton, P. *SAE Technical Paper 1999-01-1469* **1999**.
(38) Holmén, B. A.; Niemeier, D. A. *Transportation Res., Part D., Transport Environ.* **1998**, *3*, 117−128.
(39) Tobias, H. J.; Beving, D. E.; Ziemann, P. J.; Sakurai, H.; Zuk, M.; McMurry, P. H.; Zarling, D.; Waytulonis, R.; Kittelson, D. B. *Environ. Sci. Technol.* **2001**, *35*, 2233−2243.
(40) Kittelson, D. B.; Arnold, M.; Watts, W. F., Jr. *Review of Diesel Particulate Matter Sampling Methods, Final Report*; University of Minnesota, 1999.
(41) Harrison, R. M.; Jones, M.; Collins, G. *Atmos. Environ.* **1999**, *33*, 309−321.
(42) Hitchins, J.; Morawska, L.; Wolff, R.; Gilbert, D. *Atmos. Environ.* **2000**, *34*, 51−59.
(43) Nanzetta, M. K.; Holmén, B. A. *Air Waste Management Association Annual Conference* **2001**, *Paper #209*.
(44) Shi, J. P.; Evans, D. E.; Khan, A. A.; Harrison, R. M. *Atmos. Environ.* **2001**, *35*, 1193−1202.

Received for review December 29, 2001. Revised manuscript received September 9, 2002. Accepted September 10, 2002.

ES015884G